

Nonreciprocal single-photon frequency converter via multiple semi-infinite coupled-resonator waveguides

Xun-Wei Xu,^{1,*} Ai-Xi Chen,^{2,1,†} Yong Li,^{3,4,5} and Yu-xi Liu^{6,7}

¹*Department of Applied Physics, East China Jiaotong University, Nanchang, 330013, China*

²*Department of Physics, Zhejiang Sci-Tech University, Hangzhou, 310018, China*

³*Beijing Computational Science Research Center, Beijing 100193, China*

⁴*Synergetic Innovation Center of Quantum Information and Quantum Physics,
University of Science and Technology of China, Hefei 230026, China*

⁵*Synergetic Innovation Center for Quantum Effects and Applications, Hunan Normal University, Changsha 410081, China*

⁶*Institute of Microelectronics, Tsinghua University, Beijing 100084, China*

⁷*Tsinghua National Laboratory for Information Science and Technology (TNList), Beijing 100084, China*

(Dated: September 25, 2018)

We propose to construct a nonreciprocal single-photon frequency converter via multiple semi-infinite coupled-resonator waveguides (CRWs). We first demonstrate that the frequency of a single photon can be converted nonreciprocally through two CRWs, which are coupled indirectly by optomechanical interactions with two nondegenerate mechanical modes. Based on such nonreciprocity, two different single-photon circulators are proposed in the T-shaped waveguides consisting of three semi-infinite CRWs, which are coupled in pairwise by optomechanical interactions. One circulator is proposed by using two nondegenerate mechanical modes and the other one is proposed by using three nondegenerate mechanical modes. Nonreciprocal single-photon frequency conversion is induced by breaking the time-reversal symmetry, and the optimal conditions for nonreciprocal frequency conversion are obtained. These proposals can be used to realize nonreciprocal frequency conversion of single photons in any two distinctive waveguides with different frequencies and they can allow for dynamic control of the direction of frequency conversion by tuning the phases of external driving lasers, which may have versatile applications in hybrid quantum networks.

I. INTRODUCTION

To build a hybrid quantum network, by harnessing advantages of different systems [1, 2], we have to tackle an important problem: how to integrate different components that don't operate at the same frequency. One solution is to build a photon frequency converter which converts the input photons of one frequency into the output photons of another frequency. Traditionally, photon frequency conversion is demonstrated by three-wave mixing in second-order nonlinear materials [3–9] or four-wave mixing in third-order nonlinear materials [10–12]. With the development of circuit quantum electrodynamics, frequency conversion was even proposed in a single three-level superconducting quantum circuit by three-wave mixing [13, 14] or a single qubit in the ultrastrong coupling regime [15]. Moreover, single-photon frequency converters have been proposed in the one-dimensional (1D) linear waveguide [16–18] or 1D coupled-resonator waveguides (CRWs) [19, 20] with a three-level system coupled to different channels. Since the mechanical resonators can be coupled to various electromagnetic fields with distinctively different wavelengths through radiation pressure (for reviews, see Refs. [21–25]), frequency conversion has been demonstrated via two optical cavities with different frequencies, coupled by a single mechanical resonator via optomechanical interactions [26–32]. Recently, the conversion between microwave and optical frequencies has been implemented in the electro-

optomechanical systems [33–36].

Besides frequency converters, isolators and circulators are also dispensable elements in constructing hybrid quantum networks for protecting some elements from unwanted noises or retracing fields [37]. It is well known that, the systems with broken time-reversal symmetry can be used to construct isolators or circulators. In recent years, as a non-magnetic strategy, optical nonreciprocity in the coupled cavity modes with relative phase has drawn more and more attentions, and many different structures have been proposed theoretically [38–49] and demonstrated experimentally [50, 51].

In a recent work, we have proposed a nonreciprocal frequency converter in an electro-optomechanical system with a microwave mode and an optical mode, coupled indirectly via two nondegenerate mechanical modes [52]. Due to the broken time-reversal symmetry, the nonreciprocity is obtained when the transmission of photons from one mode to the other one is enhanced for constructive quantum interference while the transmission in the reversal direction is suppressed with destructive quantum interference. Based on a similar mechanism, nonreciprocal frequency conversion was explored theoretically [53–55] and realized experimentally [56–58] in many different systems.

In this paper, we propose a nonreciprocal single-photon frequency converter, consisting of two or three 1D semi-infinite CRWs with different frequencies, which are coupled indirectly by nondegenerate mechanical modes via optomechanical interactions. In quantum networks, this system can also be viewed as quantum channels (1D semi-infinite CRWs) connected by a quantum node (the optomechanical systems [52]). Different from the previous studies on nonreciprocal frequency conversion [52–56], we consider the dispersion rela-

*Electronic address: davidxu0816@163.com

†Electronic address: aixichen@ecjtu.edu.cn

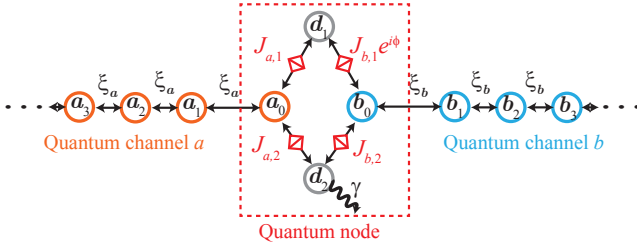


FIG. 1: (Color online) Schematic diagram of a waveguide consisting of two semi-infinite CRWs (a_j and b_j for $j \geq 0$) with different frequencies (e.g., one is optical CRW and the other one is microwave CRW) coupled indirectly by the two mechanical modes (d_1 and d_2).

tions of the quantum channels, which play an important role in single-photon frequency conversion. Also unlike the previous studies on single-photon nonreciprocity in 1D CRWs [59–61], in this work, the frequencies of the CRWs are very different and they can not be coupled together directly. The addition of optomechanical systems (or mechanical modes) to the frequency converter offers the possibility to enable nonreciprocal frequency transduction between two CRWs with distinctively different frequencies and allows for dynamic control of the direction of frequency conversion by tuning the phases of external driving lasers.

The paper is organized as follows: In Sec. II, we propose a single-photon frequency converter using two CRWs, coupled indirectly by two nondegenerate mechanical modes via optomechanical interactions. In Secs. III and IV, two different single-photon circulators are proposed in the T-shaped waveguides consisting of three semi-infinite CRWs, which are mutually coupled by optomechanical interactions. One circulator uses two nondegenerate mechanical modes and the other one uses three nondegenerate mechanical modes. Finally, we summarize our results in Sec. V.

II. NONRECIPROCAL SINGLE-PHOTON FREQUENCY CONVERTER

A. Theoretical model and scattering matrix

As schematically shown in Fig. 1, a waveguide consists of two semi-infinite coupled-resonator waveguides (CRWs) with different frequencies (e.g., one is optical CRW and the other one is microwave CRW), in which both end side cavities are coupled to two mechanical modes via optomechanical interactions. The semi-infinite CRWs, as quantum channels for single-photon transmission, are made by infinite identical single-mode cavities, which are coupled to each other through coherent hopping of photons between neighboring cavities [62–65]. The two end side cavities (a_0 and b_0), coupled indirectly by the two mechanical modes (d_1 and d_2), are served as a quantum node for single-photon frequency conversion. The total system can be described by the Hamiltonian

$$H_0 = \sum_{l=a,b} H_l + H_m + H_{\text{int}} \quad (1)$$

with the Hamiltonian $\sum_{l=a,b} H_l$ for the two CRWs

$$H_l = \sum_{j=0}^{+\infty} \left[\omega_l l_j^\dagger l_j - \xi_l \left(l_j^\dagger l_{j+1} + \text{H.c.} \right) \right], \quad (2)$$

the Hamiltonian H_m for the mechanical modes

$$H_m = \omega_1 d_1^\dagger d_1 + \omega_2 d_2^\dagger d_2, \quad (3)$$

and the interaction terms H_{int} for single-photon frequency conversion

$$\begin{aligned} H_{\text{int}} = & \left(g_{a,1} a_0^\dagger a_0 + g_{b,1} b_0^\dagger b_0 \right) \left(d_1 + d_1^\dagger \right) \\ & + \left(g_{a,2} a_0^\dagger a_0 + g_{b,2} b_0^\dagger b_0 \right) \left(d_2 + d_2^\dagger \right) \\ & + \sum_{l=a,b} \sum_{i=1}^2 \left(l_0 \Omega_{l,i} e^{i\omega_{l,i} t} + \text{H.c.} \right), \end{aligned} \quad (4)$$

where l_j (l_j^\dagger , $l = a, b$) is the bosonic annihilation (creation) operator of the j th cavity with the same resonant frequency ω_l and the same coupling strength ξ_l between two nearest neighboring cavities in the CRW- l . ω_i ($i = 1, 2$) is the resonant frequency of the mechanical mode with the bosonic annihilation (creation) operator d_i (d_i^\dagger). $g_{l,i}$ is the optomechanical coupling strength between cavity l_0 ($l_0 = a_0, b_0$) and mechanical mode d_i ($d_i = d_1, d_2$). The cavity a_0 (b_0) is driven by a two-tone laser at frequencies $\omega_{a,1} = \omega_a - \omega_1 + \Delta_{a,1}$ and $\omega_{a,2} = \omega_a - \omega_2 + \Delta_{a,2}$ ($\omega_{b,1} = \omega_b - \omega_1 + \Delta_{b,1}$ and $\omega_{b,2} = \omega_b - \omega_2 + \Delta_{b,2}$) with amplitudes $\Omega_{a,1}$ and $\Omega_{a,2}$ ($\Omega_{b,1}$ and $\Omega_{b,2}$). For simplicity, we assume that $\Delta_1 \equiv \Delta_{a,1} = \Delta_{b,1}$ and $\Delta_2 \equiv \Delta_{a,2} = \Delta_{b,2}$. Thus the operators for the cavity modes can be rewritten as the sum of the quantum fluctuation operators and classical mean values, i.e., $a_j \rightarrow a_j + \sum_{i=1}^2 \alpha_{j,i}^a e^{-i\omega_{a,i} t}$ and $b_j \rightarrow b_j + \sum_{i=1}^2 \alpha_{j,i}^b e^{-i\omega_{b,i} t}$, where a_j and b_j on the right side of the arrow symbols describe the quantum fluctuation operators of the cavity modes, and the classical amplitude $\alpha_{j,i}^l$ is determined by the amplitudes $\Omega_{l,i}$, the frequency $\omega_{l,i}$, the damping rates $\kappa_{a,j}$ and $\kappa_{b,j}$ of the cavities and the damping rates γ_1 and γ_2 of the mechanical modes.

To obtain a linearized Hamiltonian, we assume that the external driving is strong, i.e. $|\alpha_{0,i}^l| \gg 1$, the system works in the resolved-sideband limit with respect to both mechanical modes, i.e. $\min\{\omega_1, \omega_2\} \gg \max\{\kappa_{a,j}, \kappa_{b,j}\}$, and the two mechanical modes are well separated in frequency, i.e. $\min\{\omega_1, \omega_2, |\omega_1 - \omega_2|\} \gg \max\{|g_{l,i} \alpha_{0,i}^l|, \gamma_1, \gamma_2\}$. After making the standard linearization under the rotating-wave approximation, in the rotating reference frame with respect to $H_{\text{rot}} = \sum_{l=a,b} \sum_{j=0}^{+\infty} \omega_l l_j^\dagger l_j + \sum_{i=1,2} (\omega_i - \Delta_i) d_i^\dagger d_i$, the linearized Hamiltonian with time-independent terms becomes

$$H_{\text{fc}} = \sum_{l=a,b} H_l + H_m + H_{\text{int}}, \quad (5)$$

where H_l , H_m , and H_{int} are replaced by

$$H_l = -\xi_l \sum_{j=0}^{+\infty} \left(l_j^\dagger l_{j+1} + \text{H.c.} \right), \quad (6)$$

$$H_m = \Delta_1 d_1^\dagger d_1 + \Delta_2 d_2^\dagger d_2, \quad (7)$$

$$\begin{aligned} H_{\text{int}} = & J_{a,1}(a_0^\dagger d_1 + a_0 d_1^\dagger) \\ & + J_{b,1}(e^{-i\phi} b_0^\dagger d_1 + e^{i\phi} b_0 d_1^\dagger) \\ & + J_{a,2}(a_0^\dagger d_2 + a_0 d_2^\dagger) \\ & + J_{b,2}(b_0^\dagger d_2 + b_0 d_2^\dagger). \end{aligned} \quad (8)$$

Here $J_{l,i}e^{i\phi_{l,i}} = g_{l,i}\alpha_{0,i}^l$ is the effective optomechanical coupling strength between the cavity l_0 ($l_0 = a_0, b_0$) and mechanical mode d_i ($d_i = d_1, d_2$) with real strength $J_{l,i} = |g_{l,i}\alpha_{0,i}^l|$ and phase $\phi_{l,i}$. As only the total phase $\phi = \phi_{a,1} + \phi_{a,2} + \phi_{b,1} + \phi_{b,2}$ has physical effects, without loss of generality, ϕ is only kept in the terms of $b_0 d_1^\dagger$ and $b_0^\dagger d_1$ in Eq. (8) and the following derivation. It should be noted that ϕ and $J_{l,i}$ are dynamically tunable parameters, which can be controlled by tuning the strengths and phases of the external driving fields. The time-reversal symmetry of the whole system is broken when we choose the phase $\phi \neq n\pi$ (n is an integer). As we will show later, the direction of frequency conversion can be controlled dynamically by tuning the value of the total phase ϕ .

In this paper, we assume that the damping rates of the cavities in the CRWs are much smaller than the coupling strength between two nearest neighboring cavities and the effective optomechanical coupling strength, i.e. $\{\xi_l, J_{l,i}\} \gg \max\{\kappa_{a,j}, \kappa_{b,j}\}$, so that we can only consider the coherent scattering in the CRWs. Moreover, we assume that $\{\xi_l, J_{l,i}, \gamma_2\} \gg \gamma_1$, so that γ_1 can be neglected in the following calculations and the Hamiltonian for two mechanical modes with $\gamma \equiv \gamma_2$ is described by

$$H_m = \Delta_1 d_1^\dagger d_1 + (\Delta_2 - i\gamma) d_2^\dagger d_2. \quad (9)$$

The mechanical damping rate γ can be controlled by coupling the mechanical mode to an auxiliary cavity [66–69], and a suitable mechanical damping is another crucial condition to obtain desired nonreciprocal single-photon frequency conversion in this model [59].

To derive the scattering matrix between different CRWs, we consider the stationary eigenstate of a single photon in the whole system as

$$\begin{aligned} |E\rangle = & \sum_{j=0}^{+\infty} [u_a(j) a_j^\dagger |0\rangle + u_b(j) b_j^\dagger |0\rangle] \\ & + u_{d1} d_1^\dagger |0\rangle + u_{d2} d_2^\dagger |0\rangle, \end{aligned} \quad (10)$$

where $|0\rangle$ indicates the vacuum state of the whole system, $u_l(j)$ denotes the probability amplitude in the state with a single photon in the j th cavity of the CRW- l , and u_{d1} (u_{d2}) denotes the probability amplitude with a single phonon in the mechanical mode d_1 (d_2). The dispersion relation of the semi-infinite CRW- l in the rotating reference frame is given by [19]

$$E_l = -2\xi_l \cos k_l, \quad 0 < k_l < \pi, \quad (11)$$

where E_l is the energy and k_l is the wave number of the single photon in the CRW- l . Without loss of generality, we assume that $\xi_l > 0$. Substituting the stationary eigenstate in

Eq. (10) and the Hamiltonian in Eq. (5) into the eigenequation $H_{\text{fc}}|E\rangle = E|E\rangle$, we can obtain the coupled equations for the probability amplitudes as

$$J_{a,1}u_{d1} + J_{a,2}u_{d2} - \xi_a u_a(1) = E u_a(0), \quad (12)$$

$$J_{b,1}e^{-i\phi}u_{d1} + J_{b,2}u_{d2} - \xi_b u_b(1) = E u_b(0), \quad (13)$$

$$J_{a,1}u_a(0) + J_{b,1}e^{i\phi}u_b(0) = (E - \Delta_1)u_{d1}, \quad (14)$$

$$J_{a,2}u_a(0) + J_{b,2}u_b(0) = (E - \Delta_2 + i\gamma)u_{d2}, \quad (15)$$

$$E u_l(j) + \xi_l u_l(j+1) + \xi_l u_l(j-1) = 0 \quad (16)$$

with $j > 0$ and $l = a, b$.

If a single photon with energy E is incident from the infinity side of CRW- l , the photon-phonon interactions in the quantum node will result in photon scattering between different CRWs or photon absorption by the dissipative mechanical mode. The general expressions of the probability amplitudes in the CRWs ($j \geq 0$) are given by

$$u_l(j) = e^{-ik_l j} + s_{ll} e^{ik_l j}, \quad (17)$$

$$u_{l'}(j) = s_{l'l} e^{ik_{l'} j}, \quad (18)$$

where $s_{l'l}$ denotes the single-photon scattering amplitude from CRW- l to CRW- l' ($l, l' = a, b$). Substituting Eqs. (17) and (18) into Eqs. (12)-(16), then we obtain the scattering matrix as

$$S = \begin{pmatrix} s_{aa} & s_{ab} \\ s_{ba} & s_{bb} \end{pmatrix}, \quad (19)$$

where

$$s_{aa} = D^{-1} [J_{ab}J_{ba} - (\xi_a e^{ik_a} + \Delta_a) (\xi_b e^{-ik_b} + \Delta_b)], \quad (20)$$

$$s_{ba} = i2D^{-1} J_{ba} \xi_a \sin k_a, \quad (21)$$

$$s_{ab} = i2D^{-1} J_{ab} \xi_b \sin k_b, \quad (22)$$

$$s_{bb} = D^{-1} [J_{ab}J_{ba} - (\xi_a e^{-ik_a} + \Delta_a) (\xi_b e^{ik_b} + \Delta_b)], \quad (23)$$

$$D = (\xi_a e^{-ik_a} + \Delta_a) (\xi_b e^{-ik_b} + \Delta_b) - J_{ab}J_{ba} \quad (24)$$

with the effective coupling strengths $J_{ll'}$ and frequency shifts Δ_l induced by the two mechanical modes defined by

$$J_{ab} \equiv \frac{J_{a,1}J_{b,1}e^{i\phi}}{(E - \Delta_1)} + \frac{J_{a,2}J_{b,2}}{(E - \Delta_2 + i\gamma)}, \quad (25)$$

$$J_{ba} \equiv \frac{J_{a,1}J_{b,1}e^{-i\phi}}{(E - \Delta_1)} + \frac{J_{a,2}J_{b,2}}{(E - \Delta_2 + i\gamma)}, \quad (26)$$

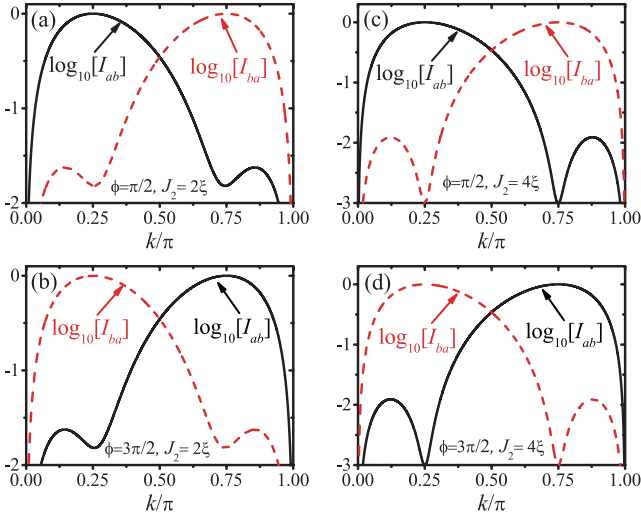


FIG. 2: (Color online) Scattering flows $\log_{10}[I_{ab}]$ (black solid curves) and $\log_{10}[I_{ba}]$ (red dashed curves) are shown as functions of the wave number k/π for: (a) $\phi = \pi/2$ and $J_2 = 2\xi$, (b) $\phi = 3\pi/2$ and $J_2 = 2\xi$, (c) $\phi = \pi/2$ and $J_2 = 4\xi$, (d) $\phi = 3\pi/2$ and $J_2 = 4\xi$. The other parameters are $J_1 = \xi$, $\Delta_1 = \Delta_2 = 0$, and γ is obtained from Eq. (32).

$$\Delta_a \equiv \frac{(J_{a,1})^2}{(E - \Delta_1)} + \frac{(J_{a,2})^2}{(E - \Delta_2 + i\gamma)}, \quad (27)$$

$$\Delta_b \equiv \frac{(J_{b,1})^2}{(E - \Delta_1)} + \frac{(J_{b,2})^2}{(E - \Delta_2 + i\gamma)}. \quad (28)$$

To quantify nonreciprocity conversion, we define the scattering flows of the single photons from CRW- l to CRW- l' as [20]

$$I_{l'l} = |s_{l'l}|^2 \frac{\xi_{l'} \sin k_{l'}}{\xi_l \sin k_l}, \quad (29)$$

where $\xi_l \sin k_l$ ($\xi_{l'} \sin k_{l'}$) is the group velocity in the CRW- l (CRW- l'). In our model, $I_{ba} \neq I_{ab}$ implies the appearance of nonreciprocal single-photon frequency conversion, and the perfect nonreciprocal single-photon frequency conversion is obtained when $I_{ba} = 1$ and $I_{ab} = 0$, or $I_{ba} = 0$ and $I_{ab} = 1$.

B. Nonreciprocal single-photon frequency converter

Before the numerical calculations of the scattering flows I_{ab} and I_{ba} , it is instructive to find the optimal conditions for nonreciprocal single-photon frequency conversion analytically. For simplicity, we assume that the detunings $\Delta_1 = \Delta_2 = 0$, the two CRWs have the same parameters (i.e., $\xi \equiv \xi_a = \xi_b$, and $k \equiv k_a = k_b$) and they are symmetrically coupled to the two mechanical modes ($J_1 \equiv J_{a,1} = J_{b,1}$, $J_2 \equiv J_{a,2} = J_{b,2}$) with $J_1 = \xi$. Under the condition that $\gamma \gg \xi$, the optimal conditions for nonreciprocal single-photon frequency conversion obtained from Eqs. (20)-(24) are

$$\phi \approx \frac{\pi}{2} \quad \text{or} \quad \frac{3\pi}{2}, \quad (30)$$

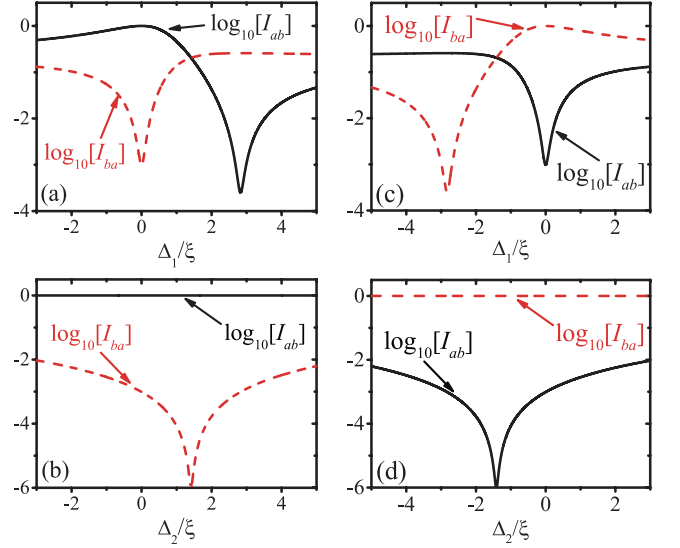


FIG. 3: (Color online) Scattering flows $\log_{10}[I_{ab}]$ (black solid curves) and $\log_{10}[I_{ba}]$ (red dashed curves) are plotted as functions of Δ_1/ξ in (a) and (c), and as functions of Δ_2/ξ in (b) and (d) with wave numbers: (a) and (b) $k = \pi/4$, (c) and (d) $k = 3\pi/4$. The other parameters are $\phi = \pi/2$, $J_1 = \xi$, $J_2 = 4\xi$, and γ is obtained from Eq. (32).

$$k \approx \frac{\pi}{4} \quad \text{or} \quad \frac{3\pi}{4}, \quad (31)$$

$$\frac{\gamma}{\xi} \approx \sqrt{2 \left(\frac{J_2}{\xi} \right)^4 + 2}. \quad (32)$$

In order to satisfy the condition $\gamma \gg \xi$, we should choose $J_2 \gg \xi$ in Eq. (32).

Scattering flows I_{ab} (black solid curve) and I_{ba} (red dashed curve) as functions of the wave number k/π are shown in Fig. 2. The optimal nonreciprocity appears around the point $k \approx \pi/4$ and $3\pi/4$ for $\phi \approx \pi/2$ or $3\pi/2$, which exhibits good agreement with the analytical result shown in Eqs. (30) and (31). Specifically, when $\phi = \pi/2$, in Figs. 2(a) and 2(c), we show the reciprocal transmission from CRW- b to CRW- a (CRW- a to CRW- b) at $k \approx \pi/4$ ($k \approx 3\pi/4$). In contrast, when $\phi = 3\pi/2$, we see the reciprocal transmission from CRW- a to CRW- b (CRW- b to CRW- a) at $k \approx \pi/4$ ($k \approx 3\pi/4$). These imply that we can reverse the direction of frequency conversion by tuning the phase from $\phi = \pi/2$ to $\phi = 3\pi/2$. Scattering flows I_{ab} and I_{ba} for different J_2 are shown in Figs. 2(a) and 2(c) [or Figs. 2(b) and 2(d)], which demonstrate that the nonreciprocity of the system improves dramatically if we take a larger value of J_2/ξ (as well as γ/ξ).

The optimal conditions for nonreciprocal single-photon frequency conversion given in Eqs. (30)-(32) are only applicable for zero frequency detunings $\Delta_1 = \Delta_2 = 0$. The following discussions based on numerical calculations will show the effects of the frequency detunings (Δ_1 and Δ_2) on frequency conversion. Scattering flows I_{ab} (black solid curve) and I_{ba} (red dashed curve) as functions of the detunings Δ_1/ξ and

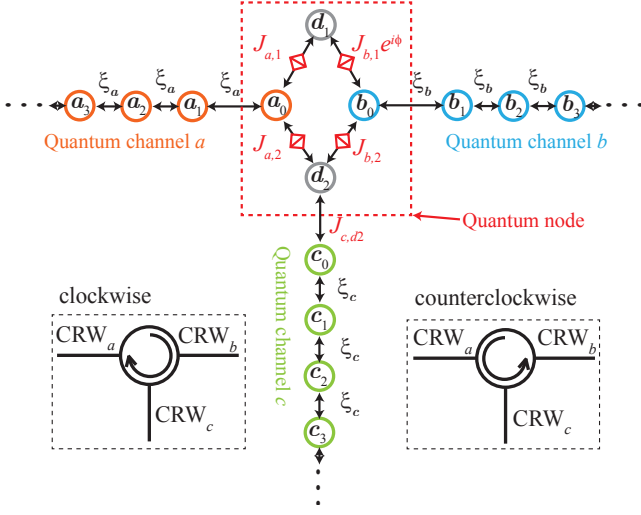


FIG. 4: (Color online) Schematic diagram of a T-shaped waveguide consisting of three semi-infinite CRWs (a_j , b_j and c_j for $j \geq 0$) coupled indirectly by two mechanical modes (d_1 and d_2).

Δ_2/ξ are shown in Fig. 3. From these figures, we can see two interesting phenomena. (i) Besides $\Delta_1 = 0$, there is another optimal detuning $\Delta_1 = 2\sqrt{2}\xi$ ($\Delta_1 = -2\sqrt{2}\xi$) for observing nonreciprocity in the oppose direction with the wave number $k = \pi/4$ ($k = 3\pi/4$). Thus we can change the direction of the scattering flows from $b \rightarrow a$ to $a \rightarrow b$ (from $a \rightarrow b$ to $b \rightarrow a$) by tuning the detuning from $\Delta_1 = 0$ to $\Delta_1 = 2\sqrt{2}\xi$ ($\Delta_1 = -2\sqrt{2}\xi$). This phenomenon can be simply understood by plugging $\Delta_1 = 2\sqrt{2}\xi$ and $k = \pi/4$ ($\Delta_1 = -2\sqrt{2}\xi$ and $k = 3\pi/4$) into Eqs. (21) and (22), then we obtain $I_{ab} \approx 0$ and $I_{ba} \approx 0.258$ ($I_{ba} \approx 0$ and $I_{ab} \approx 0.258$) for $\phi = \pi/2$. (ii) We can improve the nonreciprocity by taking $\Delta_2 = \sqrt{2}\xi$ for $k = \pi/4$ ($\Delta_2 = -\sqrt{2}\xi$ for $k = 3\pi/4$). This phenomenon corresponds to the condition $E = \Delta_2$ for $k = \pi/4$ (or $k = 3\pi/4$) in Eqs. (25)-(28), so that the optimal phase is $\phi = \pi/2$ (or $\phi = 3\pi/2$).

III. SINGLE-PHOTON CIRCULATOR IN T-SHAPED WAVEGUIDE

A. Theoretical model and scattering matrix

Based on the nonreciprocal single-photon frequency conversion discussed in Sec. II, we propose a three-port single-photon circulator in a dissipation-free T-shaped waveguide, i.e. $\gamma = 0$, as schematically shown in Fig. 4, which is made up by coupling an additional semi-infinite CRW (CRW- c) to the mechanical mode d_2 in Fig. 1 through optomechanical interaction. The T-shaped waveguide can be described by the Hamiltonian

$$H_{T,I} = H_0 + H_c + H_{c,int}, \quad (33)$$

where H_0 is given in Eq. (1), and the two additional terms H_c and $H_{c,int}$ are

$$H_c = \sum_{j=0}^{+\infty} \left[\omega_c c_j^\dagger c_j - \xi_c \left(c_j^\dagger c_{j+1} + \text{H.c.} \right) \right], \quad (34)$$

$$H_{c,int} = g_{c,2} c_0^\dagger c_0 \left(d_2 + d_2^\dagger \right) + \left(c_0 \Omega_{c,2} e^{i\omega_c t} + \text{H.c.} \right). \quad (35)$$

Here c_j (c_j^\dagger) is the bosonic annihilation (creation) operator of the j th cavity with the same resonant frequency ω_c and the same coupling strength ξ_c between two nearest neighboring cavities in the CRW- c . $g_{c,2}$ is the optomechanical coupling strength between the cavity c_0 and the mechanical mode d_2 . Cavity c_0 is driven by a laser at frequency $\omega_{c,2} = \omega_c - \omega_2 + \Delta_{c,2}$ with $\Delta_2 = \Delta_{c,2}$ and amplitude $\Omega_{c,2}$. Similarly, the operator for the cavity c_j can also be rewritten as the sum of its quantum fluctuation operator and classical mean value as $c_j \rightarrow c_j + \alpha_{j,2}^c e^{-i\omega_c t}$, where the classical amplitude $\alpha_{j,2}^c$ is determined by the amplitude $\Omega_{c,2}$, the frequency $\omega_{c,2}$, the damping rates $\kappa_{a,j}$, $\kappa_{b,j}$ and $\kappa_{c,j}$ of the cavities and the mechanical damping rates γ_1 and γ_2 .

To obtain a linearized Hamiltonian, we assume that the external driving is strong, i.e. $|\alpha_{0,i}^l| \gg 1$, the system works in the resolved-sideband limit with respect to both mechanical modes, i.e. $\min\{\omega_1, \omega_2\} \gg \max\{\kappa_{a,j}, \kappa_{b,j}, \kappa_{c,j}\}$, and the two mechanical modes are well separated in frequency, i.e. $\min\{\omega_1, \omega_2, |\omega_1 - \omega_2|\} \gg \max\{|\omega_{l,i} \alpha_{0,i}^l|, \gamma_1, \gamma_2\}$. After making the standard linearization under the rotating-wave approximation, in the rotating reference frame with respect to $H_{\text{rot}} = \sum_{l=a,b,c} \sum_{j=0}^{+\infty} \omega_l l_j^\dagger l_j + \sum_{i=1,2} (\omega_i - \Delta_i) d_i^\dagger d_i$, the linearized Hamiltonian for the T-shaped waveguide is described by

$$H_{\text{cir,I}} = \sum_{l=a,b,c} H_l + H_m + H_{\text{int,I}}, \quad (36)$$

where H_l and H_m have been given in Eqs. (6) and (7), and the interaction term $H_{\text{int,I}}$ is given by

$$\begin{aligned} H_{\text{int,I}} = & J_{a,1} \left(a_0^\dagger d_1 + a_0 d_1^\dagger \right) \\ & + J_{b,1} \left(e^{-i\phi} b_0^\dagger d_1 + e^{i\phi} b_0 d_1^\dagger \right) \\ & + J_{a,2} \left(a_0^\dagger d_2 + a_0 d_2^\dagger \right) \\ & + J_{b,2} \left(b_0^\dagger d_2 + b_0 d_2^\dagger \right) \\ & + J_{c,2} \left(c_0^\dagger d_2 + c_0 d_2^\dagger \right). \end{aligned} \quad (37)$$

Here $J_{c,2} = |g_{c,2} \alpha_{0,2}^c|$ is the effective optomechanical coupling strength between the cavity c_0 and mechanical mode d_2 . We assume that the damping rates $\kappa_{l,j}$ of the cavities in the CRWs and the damping rates γ_i of the mechanical modes are much smaller than the coupling strengths between two nearest neighboring cavities and the effective optomechanical coupling strengths, i.e. $\{\xi_l, J_{l,i}\} \gg \max\{\kappa_{l,j}, \gamma_i\}$, so that we can only consider the coherent scattering in the CRWs.

The stationary eigenstate of a single-photon scattering in the T-shaped waveguide is given by

$$|E\rangle = \sum_{l=a,b,c} \sum_{j=0}^{+\infty} u_l(j) l_j^\dagger |0\rangle + u_{d1} d_1^\dagger |0\rangle + u_{d2} d_2^\dagger |0\rangle. \quad (38)$$

The dispersion relation of the CRW- c can be obtained from Eq. (11) by setting the superscript $l = c$. Substituting the stationary eigenstate and the Hamiltonian into the eigenequation $H_{\text{cir,I}} |E\rangle = E |E\rangle$, we can obtain the coupled equations for the probability amplitudes as in Eqs. (12)-(16) but with Eq. (15) replaced by the following two equations

$$J_{a,2} u_a(0) + J_{b,2} u_b(0) + J_{c,2} u_c(0) = (E - \Delta_2) u_{d2}, \quad (39)$$

$$J_{c,2} u_{d2} - \xi_c u_c(1) = E u_c(0), \quad (40)$$

and the subscript l in Eq. (16) is replaced by $l = a, b, c$.

If a single photon with energy E is incident from the infinity side of CRW- l , the interactions between cavity l_0 and l'_0 ($l_0, l'_0 = a_0, b_0, c_0$) mediated by two mechanical modes will result in photon scattering between different quantum channels. The general expressions for the probability amplitudes in three quantum channels ($l = a, b, c$) are given by ($j \geq 0$)

$$u_l(j) = e^{-ik_l j} + s_{ll} e^{ik_l j}, \quad (41)$$

$$u_{l'}(j) = s_{l'l} e^{ik_{l'} j}, \quad (42)$$

$$u_{l''}(j) = s_{l''l} e^{ik_{l''} j}, \quad (43)$$

where $s_{l'l}$ ($s_{l''l}$) denotes the scattering amplitude from CRW- l to CRW- l' (CRW- l''). Substituting Eqs. (41)-(43) into the coupled equations for the probability amplitudes, we can obtain the scattering matrix as

$$S = M^{-1} N, \quad (44)$$

with

$$S = \begin{pmatrix} s_{aa} & s_{ab} & s_{ac} \\ s_{ba} & s_{bb} & s_{bc} \\ s_{ca} & s_{cb} & s_{cc} \end{pmatrix}, \quad (45)$$

$$M = \begin{pmatrix} \xi'_a e^{-ik'_a} & J_{ab} e^{i\phi'} & J_{ca} \\ J_{ab} e^{-i\phi'} & \xi'_b e^{-ik'_b} & J_{bc} \\ J_{ca} & J_{bc} & \xi'_c e^{-ik'_c} \end{pmatrix}, \quad (46)$$

$$N = - \begin{pmatrix} \xi'_a e^{ik'_a} & J_{ab} e^{i\phi'} & J_{ca} \\ J_{ab} e^{-i\phi'} & \xi'_b e^{ik'_b} & J_{bc} \\ J_{ca} & J_{bc} & \xi'_c e^{ik'_c} \end{pmatrix}, \quad (47)$$

where the renormalized coupling strength ξ'_l and wave number k'_l of the single photon in the CRW- l are defined by

$$\xi'_l e^{ik'_l} \equiv \xi_l e^{ik_l} + \Delta_l. \quad (48)$$

The effective coupling strengths $J_{l'l'}$, phase ϕ' , and frequency shifts Δ_l induced by the two mechanical modes are defined by

$$J_{ab} e^{i\phi'} \equiv \frac{J_{a,1} J_{b,1} e^{i\phi}}{(E - \Delta_1)} + \frac{J_{a,2} J_{b,2}}{(E - \Delta_2)}, \quad (49)$$

$$J_{ca} \equiv \frac{J_{a,2} J_{c,2}}{(E - \Delta_2)}, \quad (50)$$

$$J_{bc} \equiv \frac{J_{b,2} J_{c,2}}{(E - \Delta_2)}, \quad (51)$$

$$\Delta_a \equiv \frac{(J_{a,1})^2}{(E - \Delta_1)} + \frac{(J_{a,2})^2}{(E - \Delta_2)}, \quad (52)$$

$$\Delta_b \equiv \frac{(J_{b,1})^2}{(E - \Delta_1)} + \frac{(J_{b,2})^2}{(E - \Delta_2)}, \quad (53)$$

$$\Delta_c \equiv \frac{(J_{c,2})^2}{(E - \Delta_2)}. \quad (54)$$

B. Single-photon circulator

Let us give the optimal conditions for observing perfect circulators first. A perfect circulator is obtained when we have $I_{ba} = I_{cb} = I_{ac} = 1$ or $I_{ab} = I_{bc} = I_{ca} = 1$ and the other scattering flows are equal to zero. For the sake of simplicity, we assume that the detunings $\Delta_1 = \Delta_2 = 0$, the CRW- a and CRW- b have the same parameters (i.e. $\xi \equiv \xi_a = \xi_b$, $k \equiv k_a = k_b$), and they are symmetrically coupled to the two mechanical modes (i.e. $J_1 \equiv J_{a,1} = J_{b,1}$, $J_2 \equiv J_{a,2} = J_{b,2}$) with the coupling strength $J_1 = \xi$. Based on these assumptions, the perfect circulator appears with parameters satisfying the optimal conditions

$$\phi = \frac{\pi}{2} \quad \text{or} \quad \frac{3\pi}{2}, \quad (55)$$

$$k = \frac{\pi}{4} \quad \text{or} \quad \frac{3\pi}{4}, \quad (56)$$

$$\frac{J_{c,2}}{\xi} = \sqrt{\left(\frac{J_2}{\xi}\right)^4 + 1}, \quad (57)$$

$$\xi_c = \left| \frac{(J_{bc})^2}{\xi e^{-ik} + \Delta_a} - \Delta_c \right|, \quad (58)$$

where J_{bc} has been given in Eq. (51).

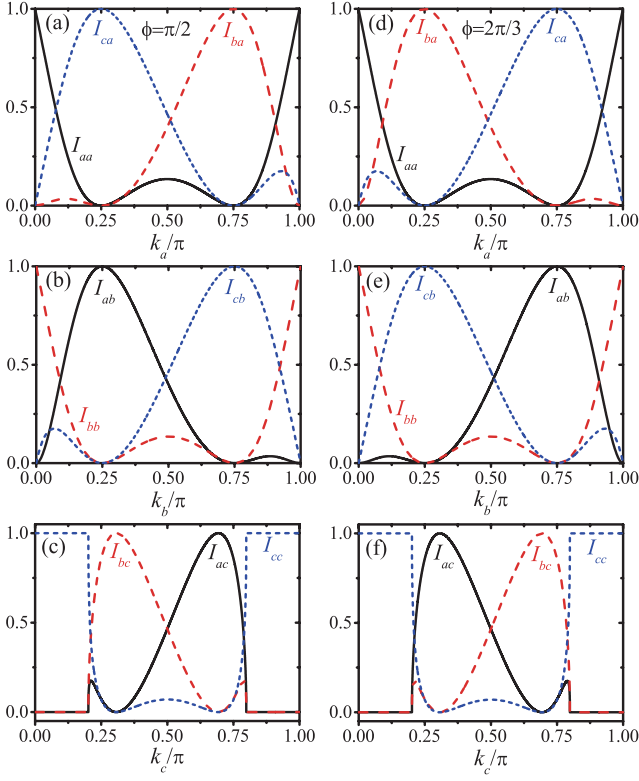


FIG. 5: (Color online) Scattering flows $I_{l'l}$ ($l, l' = a, b, c$) as functions of the wave number k_l/π of a single photon incident from CRW- l for (a)-(c) $\phi = \pi/2$ and (d)-(f) $\phi = 3\pi/2$. $J_{c,2}$ and ξ_c are obtained from Eqs. (57) and (58), and the other parameters are $\Delta_1 = \Delta_2 = 0$, $J_{a,1} = J_{b,1} = \xi$, and $J_{a,2} = J_{b,2} = 1.2\xi$.

In Fig. 5, the scattering flows $I_{l'l}$ ($l, l' = a, b, c$) are plotted as functions of the wave number k_l/π of a single photon incident from CRW- l for (a)-(c) $\phi = \pi/2$ and (d)-(f) $\phi = 3\pi/2$. As shown in Figs. 5(a)-(c), when $\phi = \pi/2$, we obtain that $I_{ba} = I_{cb} = I_{ac} = 1$ and the other scattering flows are equal to zero for the wave number $k = \pi/4$ ($k_a = k_b = k$, $k_c = \arccos[\xi \cos(k)/\xi_c]$), or obtain that $I_{ab} = I_{bc} = I_{ca} = 1$ and the other scattering flows are equal to zero for the wave number $k = 3\pi/4$ ($k_a = k_b = k$, $k_c = \arccos[\xi \cos(k)/\xi_c]$). As shown in Figs. 5(d)-(f), when $\phi = 3\pi/2$, we get $I_{ab} = I_{bc} = I_{ca} = 1$ with the other zero scattering flows for the wave number $k = \pi/4$ ($k_a = k_b = k$, $k_c = \arccos[\xi \cos(k)/\xi_c]$) or get $I_{ba} = I_{cb} = I_{ac} = 1$ with the other zero scattering flows for the wave number $k = 3\pi/4$ ($k_a = k_b = k$, $k_c = \arccos[\xi \cos(k)/\xi_c]$). In other words, when $\phi = \pi/2$, the signal is transferred from one CRW to another clockwise ($a \rightarrow b \rightarrow c \rightarrow a$) for the wave number $k = 3\pi/4$ ($k_a = k_b = k$, $k_c = \arccos[\xi \cos(k)/\xi_c]$) or counterclockwise ($a \rightarrow c \rightarrow b \rightarrow a$) for the wave number $k = \pi/4$ ($k_a = k_b = k$, $k_c = \arccos[\xi \cos(k)/\xi_c]$). In contrast, when $\phi = 3\pi/2$, the signal is transferred from one CRW to another counterclockwise ($a \rightarrow c \rightarrow b \rightarrow a$) for the wave number $k = 3\pi/4$ ($k_a = k_b = k$, $k_c = \arccos[\xi \cos(k)/\xi_c]$) or clockwise ($a \rightarrow b \rightarrow c \rightarrow a$) for the wave number $k = \pi/4$ ($k_a = k_b = k$, $k_c = \arccos[\xi \cos(k)/\xi_c]$). Thus, we can re-

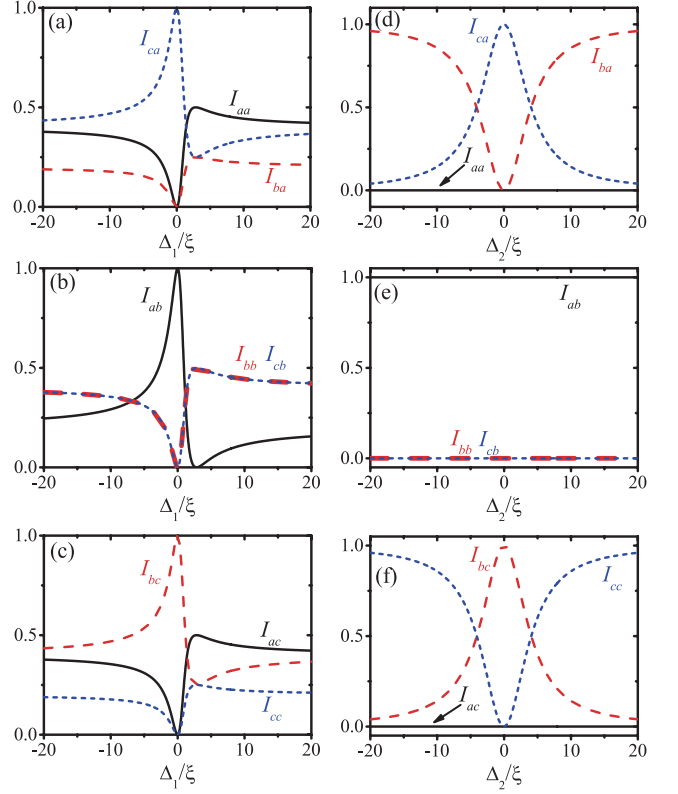


FIG. 6: (Color online) Scattering flows $I_{l'l}$ ($l, l' = a, b, c$) are plotted as functions of (a)-(c) Δ_1/ξ ($\Delta_2 = 0$) and (d)-(f) Δ_2/ξ ($\Delta_1 = 0$) for $\phi = \pi/2$ and $k = \pi/4$ ($k_a = k_b = k$, $k_c = \arccos[\xi \cos(k)/\xi_c]$). $J_{c,2}$ and ξ_c are obtained from Eqs. (57) and (58), and the other parameters are $J_{a,1} = J_{b,1} = \xi$ and $J_{a,2} = J_{b,2} = 1.2\xi$.

verse the direction of the circulator by tuning the phase from $\phi = \pi/2$ to $\phi = 3\pi/2$.

Scattering flows $I_{l'l}$ ($l, l' = a, b, c$) as functions of the detunings Δ_1/ξ and Δ_2/ξ are shown in Fig. 6. Overall, the large detunings (both Δ_1 and Δ_2) are destructive for the circulator. Similar to Fig. 3(a), when the detuning is tuned from $\Delta_1 = 0$ to $\Delta_1 = 2\sqrt{2}\xi$ as shown in Figs. 6(a)-(c), the scattering flows I_{ba} and I_{ab} change from ($I_{ba} = 0$, $I_{ab} = 1$) to ($I_{ba} = 0.25$, $I_{ab} = 0$), i.e., the direction of the scattering flows change from $b \rightarrow a$ to $a \rightarrow b$. What's more, when $I_{ab} = 1$ and $I_{bb} = I_{cb} = 0$ as shown in Fig. 3(e), the scattering flows I_{ab} , I_{bb} , and I_{cb} remain constant for different Δ_2 .

As shown in Eq. (58), i.e., $\xi_c \neq \xi$, the band widths of CRW- a and CRW- b are different from the band width of CRW- c , and nonreciprocity ($I_{l'l} \neq I_{l'l'}$) can only be obtained in the overlap band regime between the three CRWs. As shown in Fig. 5(c) and 5(f), the single photon incident from the infinity side of CRW- c will be reflected totally ($I_{cc} = 1$) in the regimes of $0 < k_c < \arccos(\xi/\xi_c)$ and $\pi - \arccos(\xi/\xi_c) < k_c < \pi$. Moreover, as shown in Eqs. (55) and (56), we can have perfect circulator only with wave number $k = \pi/4$ and $k = 3\pi/4$ for $\phi = \pi/2$ or $3\pi/2$. To improve tunability of the circulator, e.g., the perfect circulator can be obtained with the wave number in a tunable regime, we can use one more mechanical mode

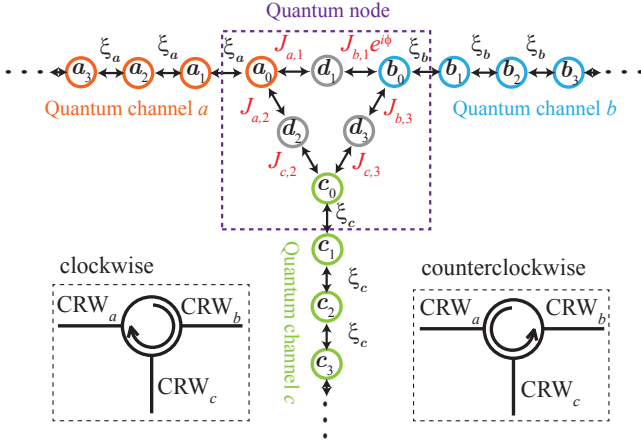


FIG. 7: (Color online) Schematic diagram of a T-shaped waveguide consisting of three semi-infinite CRWs (a_j , b_j and c_j for $j \geq 0$) coupled indirectly by three mechanical modes (d_1 , d_2 and d_3).

to connect the three CRWs and this is the focus of the next section.

IV. SINGLE-PHOTON CIRCULATOR WITH THREE MECHANICAL MODES

A. Theoretical model and scattering matrix

In this section, we propose another single-photon circulator by a different T-shaped waveguide, schematically shown in Fig. 4, which is made up of three semi-infinite CRWs coupled indirectly by three mechanical modes via optomechanical interactions. The T-shaped waveguide can be described by the Hamiltonian

$$H_{T,\text{II}} = \sum_{l=a,b,c} H_l + H_m + H_{\text{om,int}} + H_{\text{dri}} \quad (59)$$

with the Hamiltonian H_l for the CRWs given in Eq. (2), the Hamiltonian H_m for three mechanical modes

$$H_m = \omega_1 d_1^\dagger d_1 + \omega_2 d_2^\dagger d_2 + \omega_3 d_3^\dagger d_3, \quad (60)$$

the interactions $H_{\text{om,int}}$ mediated by three mechanical modes

$$\begin{aligned} H_{\text{om,int}} = & \left(g_{a,1} a_0^\dagger a_0 + g_{b,1} b_0^\dagger b_0 \right) \left(d_1 + d_1^\dagger \right) \\ & + \left(g_{a,2} a_0^\dagger a_0 + g_{c,2} c_0^\dagger c_0 \right) \left(d_2 + d_2^\dagger \right) \\ & + \left(g_{b,3} b_0^\dagger b_0 + g_{c,3} c_0^\dagger c_0 \right) \left(d_3 + d_3^\dagger \right), \quad (61) \end{aligned}$$

and the externally driving terms

$$\begin{aligned} H_{\text{dri}} = & \sum_{i=1,2} a_0 \Omega_{a,i} e^{i\omega_{a,i}t} + \sum_{i=1,3} b_0 \Omega_{b,i} e^{i\omega_{b,i}t} \\ & + \sum_{i=2,3} c_0 \Omega_{c,i} e^{i\omega_{c,i}t} + \text{H.c.}, \quad (62) \end{aligned}$$

where ω_i ($i = 1, 2, 3$) is the resonant frequency of i th mechanical mode with the bosonic annihilation (creation) operator d_i (d_i^\dagger). $g_{l,i}$ with $l = a, b, c$ is the optomechanical coupling strength between cavity l_0 ($l_0 = a_0, b_0, c_0$) and mechanical mode d_i ($d_i = d_1, d_2, d_3$). Cavity a_0 (b_0, c_0) is driven by a two-tone laser at frequencies $\omega_{a,1} = \omega_a - \omega_1 + \Delta_{a,1}$ and $\omega_{a,2} = \omega_a - \omega_2 + \Delta_{a,2}$ ($\omega_{b,1} = \omega_b - \omega_1 + \Delta_{b,1}$ and $\omega_{b,3} = \omega_b - \omega_3 + \Delta_{b,3}$, $\omega_{c,2} = \omega_c - \omega_2 + \Delta_{c,2}$ and $\omega_{c,3} = \omega_c - \omega_3 + \Delta_{c,3}$), and the amplitudes are $\Omega_{a,1}$ and $\Omega_{a,2}$ ($\Omega_{b,1}$ and $\Omega_{b,3}$, $\Omega_{c,2}$ and $\Omega_{c,3}$). Here, we assume that the detunings satisfy the conditions $\Delta_1 \equiv \Delta_{a,1} = \Delta_{b,1}$, $\Delta_2 \equiv \Delta_{a,2} = \Delta_{c,2}$, and $\Delta_3 \equiv \Delta_{b,3} = \Delta_{c,3}$. Thus the operators for the cavity modes can be rewritten as the sum of its quantum fluctuation operators and classical mean values as $a_j \rightarrow a_j + \sum_{i=1,2} \alpha_{j,i}^a e^{-i\omega_{a,i}t}$, $b_j \rightarrow b_j + \sum_{i=1,3} \alpha_{j,i}^b e^{-i\omega_{b,i}t}$ and $c_j \rightarrow c_j + \sum_{i=2,3} \alpha_{j,i}^c e^{-i\omega_{c,i}t}$, where the classical amplitude $\alpha_{j,i}^l$ is determined by the amplitudes $\Omega_{l,i}$, the frequencies $\omega_{l,i}$, the damping rates $\kappa_{l,j}$ of the cavities, and the mechanical damping rates γ_i .

To obtain a linearized Hamiltonian, similar to the previous assumptions that the external driving is strong, i.e. $|\alpha_{0,i}^l| \gg 1$, the system works in the resolved-sideband limit with respect to all three mechanical modes, i.e. $\min\{\omega_i\} \gg \max\{\kappa_{l,j}\}$, and the three mechanical modes are well separated in frequency, i.e. $\min\{\omega_i, |\omega_i - \omega_{i \neq i}|\} \gg \max\{|g_{l,i} \alpha_{0,i}^l|, \gamma_i\}$. After doing the standard linearization under the rotating-wave approximation, in the rotating reference frame with respect to $H_{\text{rot}} = \sum_{l=a,b,c} \sum_{j=0}^{+\infty} \omega_l l_j^\dagger l_j + \sum_{i=1,2,3} (\omega_i - \Delta_i) d_i^\dagger d_i$, the linearized Hamiltonian is obtained

$$H_{\text{cir,II}} = \sum_{l=a,b,c} H_l + H_m + H_{\text{int,II}} \quad (63)$$

with the Hamiltonian H_l of the CRWs given in Eq. (6), the Hamiltonian of the mechanical modes

$$H_m = \Delta_1 d_1^\dagger d_1 + \Delta_2 d_2^\dagger d_2 + \Delta_3 d_3^\dagger d_3, \quad (64)$$

and the interaction terms

$$\begin{aligned} H_{\text{int,II}} = & J_{a,1} \left(a_0^\dagger d_1 + a_0 d_1^\dagger \right) \\ & + J_{b,1} \left(e^{-i\phi} b_0^\dagger d_1 + e^{i\phi} b_0 d_1^\dagger \right) \\ & + J_{a,2} \left(a_0^\dagger d_2 + a_0 d_2^\dagger \right) \\ & + J_{c,2} \left(c_0^\dagger d_2 + c_0 d_2^\dagger \right) \\ & + J_{b,3} \left(b_0^\dagger d_3 + b_0 d_3^\dagger \right) \\ & + J_{c,3} \left(c_0^\dagger d_3 + c_0 d_3^\dagger \right). \quad (65) \end{aligned}$$

Here $J_{l,i} e^{i\phi_{l,i}} = g_{l,i} \alpha_{0,i}^l$ with $l = a, b, c$ is the effective optomechanical coupling strength between the cavity l_0 ($l_0 = a_0, b_0, c_0$) and mechanical mode d_i ($d_i = d_1, d_2, d_3$) with real strength $J_{l,i} = |g_{l,i} \alpha_{0,i}^l|$ and phase $\phi_{l,i}$. As only the total phase $\phi = \phi_{a,1} + \phi_{a,2} + \phi_{b,1} + \phi_{b,3} + \phi_{c,2} + \phi_{c,3}$ among them has physical effects, without loss of generality, ϕ is only

kept in the terms of $b_0 d_1^\dagger$ and $b_0^\dagger d_1$ in Eq. (65) and the following derivation. Similarly, $J_{l,i}$ and ϕ can be controlled dynamically by tuning the strengths and phases of the external driving fields.

The stationary eigenstate of a single photon scattering in the T-shaped waveguide with three mechanical modes is given by

$$|E\rangle = \sum_{l=a,b,c} \sum_{j=0}^{+\infty} u_l(j) l_j^\dagger |0\rangle + \sum_{i=1}^3 u_{di} d_i^\dagger |0\rangle. \quad (66)$$

Substituting the stationary eigenstate in Eq. (66) and the Hamiltonian in Eq. (63) into the eigenequation $H_{\text{cir,II}} |E\rangle = E |E\rangle$, we can obtain the coupled equations for the probability amplitudes as

$$J_{a,1} u_{d1} + J_{a,2} u_{d2} - \xi_a u_a(1) = E u_a(0), \quad (67)$$

$$J_{b,1} e^{-i\phi} u_{d1} + J_{b,3} u_{d3} - \xi_b u_b(1) = E u_b(0), \quad (68)$$

$$J_{c,2} u_{d2} + J_{c,3} u_{d3} - \xi_c u_c(1) = E u_c(0), \quad (69)$$

$$J_{a,1} u_a(0) + J_{b,1} e^{i\phi} u_b(0) = (E - \Delta_1) u_{d1}, \quad (70)$$

$$J_{a,2} u_a(0) + J_{c,2} u_c(0) = (E - \Delta_2) u_{d2}, \quad (71)$$

$$J_{b,3} u_b(0) + J_{c,3} u_c(0) = (E - \Delta_3) u_{d3}, \quad (72)$$

and the same equation as Eq. (16) with the subscript $l = a, b, c$.

If a single photon with energy E is incident from the infinity side of CRW- l , following similar steps given in Section II, we can obtain the scattering matrix given in Eqs. (44)-(48) with the effective coupling strengths $J_{ll'}$, phase ϕ' , and frequency shifts Δ_l induced by the three mechanical modes redefined by

$$J_{ab} e^{i\phi'} \equiv \frac{J_{a,1} J_{b,1}}{(E - \Delta_1)} e^{i\phi}, \quad (73)$$

$$J_{ca} \equiv \frac{J_{a,2} J_{c,2}}{(E - \Delta_2)}, \quad (74)$$

$$J_{bc} \equiv \frac{J_{b,3} J_{c,3}}{(E - \Delta_3)}, \quad (75)$$

$$\Delta_a \equiv \frac{(J_{a,1})^2}{(E - \Delta_1)} + \frac{(J_{a,2})^2}{(E - \Delta_2)}, \quad (76)$$

$$\Delta_b \equiv \frac{(J_{b,1})^2}{(E - \Delta_1)} + \frac{(J_{b,3})^2}{(E - \Delta_3)}, \quad (77)$$

$$\Delta_c \equiv \frac{(J_{c,2})^2}{(E - \Delta_2)} + \frac{(J_{c,3})^2}{(E - \Delta_3)}. \quad (78)$$

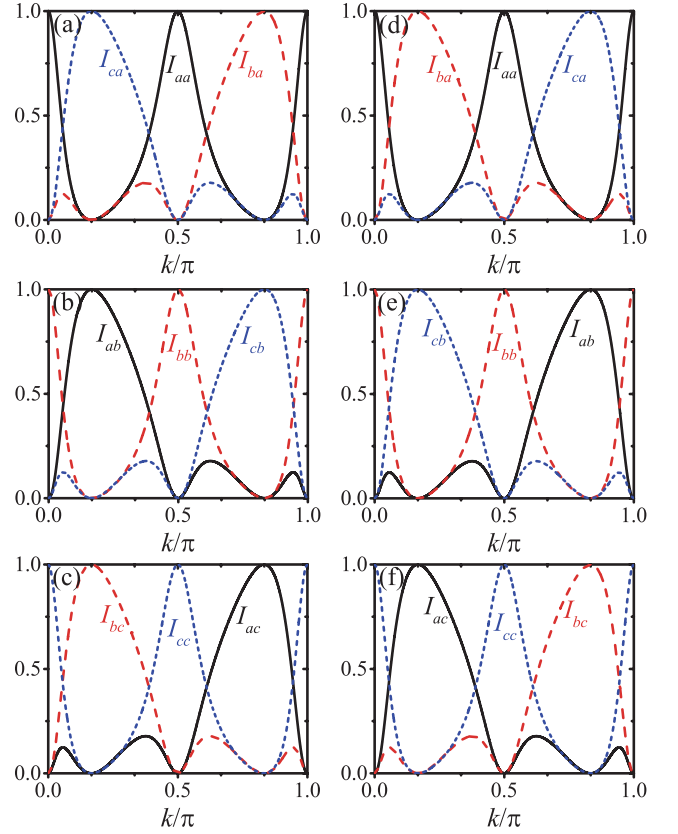


FIG. 8: (Color online) Scattering flows $I_{ll'}$ ($l, l' = a, b, c$) as functions of the wave number k/π for $\phi = \pi/3$ in (a)-(c) and $\phi = 5\pi/3$ in (d)-(f). The other parameters are $\xi_c = \xi$, $k_c = k$, $\Delta_1 = \Delta_2 = \Delta_3 = 0$, $J_1 = J_2 = J_3 = J$, and J is obtained from Eq. (79).

B. Single-photon circulator

The optimal conditions to obtain a perfect circulator can be derived analytically from Eqs. (44)-(48) [with $J_{ll'}$, ϕ' , and Δ_l defined in Eqs. (73)-(78)] by setting $I_{ba} = I_{cb} = I_{ac} = 1$ or $I_{ab} = I_{bc} = I_{ca} = 1$ and the other zero scattering flows. For the sake of simplicity, we assume that the detunings $\Delta_1 = \Delta_2 = \Delta_3 = 0$, CRW- a and CRW- b have the same parameters (i.e. $\xi \equiv \xi_a = \xi_b$, $k \equiv k_a = k_b$) with the coupling strength $J_1 \equiv J_{a,1} = J_{b,1}$, $J_2 \equiv J_{a,2} = J_{b,3}$, $J_3 \equiv J_{c,2} = J_{c,3}$. If $\xi_c = \xi$ and $J \equiv J_1 = J_2 = J_3$, the perfect circulator can be obtained when the parameters satisfy the conditions

$$\frac{J^2}{\xi^2} = \frac{2(2 - \cos \phi)}{(5 - 4 \cos \phi)}, \quad (79)$$

$$k = \frac{1}{2} \arcsin \left| \frac{4 \sin \phi - \sin 2\phi}{5 - 4 \cos \phi} \right|, \quad \text{or} \quad \pi - \frac{1}{2} \arcsin \left| \frac{4 \sin \phi - \sin 2\phi}{5 - 4 \cos \phi} \right|. \quad (80)$$

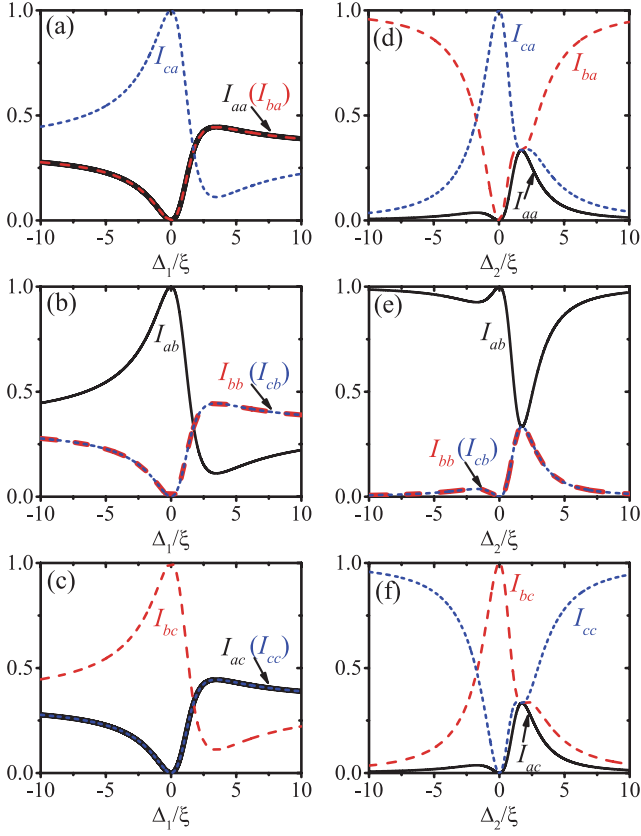


FIG. 9: (Color online) Scattering flows $I_{l'l}$ ($l, l' = a, b, c$) are plotted as functions of (a)-(c) Δ_1/ξ ($\Delta_2 = \Delta_3 = 0$) and (d)-(f) Δ_2/ξ ($\Delta_1 = 0, \Delta_3 = \Delta_2$) for $\phi = \pi/3$ and $k = 0.5236$ [obtained from Eq. (80)]. The other parameters are $\xi_c = \xi$, $k_c = k$, $J_1 = J_2 = J_3 = J$, and J is obtained from Eq. (79).

If $\xi_c \neq \xi$ and $J_1 \neq J_2 \neq J_3$, the perfect circulator can also be obtained but the conditions are changed to

$$\phi = \frac{\pi}{2} \quad \text{or} \quad \frac{3\pi}{2}, \quad (81)$$

$$k \in \left(0, \frac{\pi}{4}\right) \cup \left(\frac{3\pi}{4}, \pi\right), \quad (82)$$

and the optimal coupling strengths are given by

$$\frac{J_1}{\xi} = \sqrt{|\sin 2k|}, \quad (83)$$

$$\frac{J_2}{\xi} = \sqrt{2 \cos^2 k - |\sin 2k|}, \quad (84)$$

$$\frac{J_3}{\xi} = |\cos k|, \quad (85)$$

$$\frac{\xi_c}{\xi} = \left| \frac{\cos k}{\cos \left[\arctan \left(\frac{2 \cos^2 k - |\sin 2k|}{4 |\cos k| \sin k} \right) \right]} \right|. \quad (86)$$

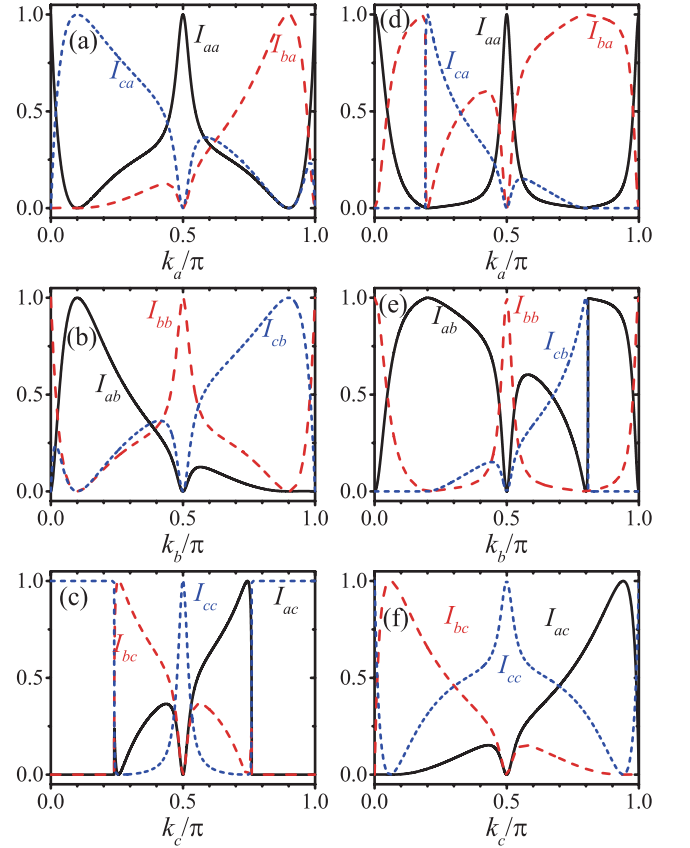


FIG. 10: (Color online) Scattering flows $I_{l'l}$ ($l, l' = a, b, c$) are plotted as functions of the wave number k_l/π of a single photon incident from CRW- l for the perfect circulator appearing at (a)-(c) $k = 0.1\pi$ and 0.9π , (d)-(f) $k = 0.2\pi$ and 0.8π . J_i ($i = 1, 2, 3$) and ξ_c are obtained from Eqs. (83)-(86), and the other parameters are $\phi = \pi/2$ and $\Delta_1 = \Delta_2 = \Delta_3 = 0$.

From Eqs. (83) and (86), if the wave number k to obtain optimal circulator satisfies the equation

$$2 \cos^2 k - |\sin 2k| = 4 \sin^2 k, \quad (87)$$

we obtain $\xi = \xi_c$ and $J_1 = J_2 = J_3$, and this is consistent with the condition given in Eq. (80) for $\phi = \pi/2$.

In Fig. 8, the scattering flows $I_{l'l}$ ($l, l' = a, b, c$) are plotted as functions of the wave number k/π for (a)-(c) $\phi = \pi/3$, (d)-(f) $\phi = 5\pi/3$ with $\xi_c = \xi$ and $J \equiv J_1 = J_2 = J_3$. As shown in Figs. 8(a)-(c), when $\phi = \pi/3$, we obtain that $I_{ab} = I_{bc} = I_{ca} = 1$ and the other scattering flows are equal to zero for wave number $k = \pi/6$, or obtain $I_{ba} = I_{cb} = I_{ac} = 1$ and the other scattering flows are equal to zero for wave number $k = 5\pi/6$. As shown in Figs. 8(d)-(f), when $\phi = 5\pi/3$, we get $I_{ba} = I_{cb} = I_{ac} = 1$ with the other zero scattering flows for wave number $k = \pi/6$, or get $I_{ab} = I_{bc} = I_{ca} = 1$ with the other zero scattering flows for wave number $k = 5\pi/6$. In other words, when $\phi = \pi/3$, the signal is transferred from one CRW to another counterclockwise ($a \rightarrow c \rightarrow b \rightarrow a$) for wave number $k = \pi/6$ or clockwise ($a \rightarrow b \rightarrow c \rightarrow a$) for wave number $k = 5\pi/6$. In contrast, when $\phi = 5\pi/3$, the signal is transferred from one CRW to another

clockwise ($a \rightarrow b \rightarrow c \rightarrow a$) for wave number $k = \pi/6$ or counterclockwise ($a \rightarrow c \rightarrow b \rightarrow a$) for wave number $k = 5\pi/6$. In other words, we can tune the phase from ϕ to $(\pi - \phi)$ to reverse the direction of the circulator.

The effects of the detunings on the single-photon transmission can be seen from Fig. 9, where the scattering flows $I_{l'l}$ ($l, l' = a, b, c$) are plotted as functions of the detunings (a)-(c) Δ_1/ξ ($\Delta_2 = \Delta_3 = 0$) and (d)-(f) Δ_2/ξ ($\Delta_1 = 0$ and $\Delta_3 = \Delta_2$). It is interesting that, we obtain $I_{l'l} = 1/3$ ($l, l' = a, b, c$) with the detunings $\Delta_1 = \sqrt{3}\xi$ ($\Delta_2 = \Delta_3 = 0$) or $\Delta_3 = \Delta_2 = \sqrt{3}\xi$ ($\Delta_1 = 0$). This interesting phenomenon can be used to design three-way single-photon beam splitter.

If we have different coupling strengths $\xi_c \neq \xi$, the band widths of CRW- a and CRW- b are different from the band width of CRW- c , and nonreciprocity ($I_{ll'} \neq I_{l'l}$) can only be obtained in the overlap band regime among the three CRWs. In Fig. 10, the scattering flows $I_{l'l}$ ($l, l' = a, b, c$) are plotted as functions of the wave number k_l/π of a single photon incident from CRW- l with different coupling strengths $\xi_c \neq \xi$. Different from the case of T-shaped waveguide with two mechanical modes as discussed in Sec. III, we can have perfect circulator with wave number $k \in (0, \pi/4) \cup (3\pi/4, \pi)$. From Eq. (87) [or Eq. (80) for $\phi = \pi/2$], to make the perfect circulator behavior appearing at $k = 0.1476\pi$ and 0.8524π , we should choose $\xi_c = \xi$ and $J_1 = J_2 = J_3$. As shown in Figs. 10(a)-(c), when the perfect circulator appears at $k = 0.1\pi$ ($< 0.1476\pi$) and 0.9π ($> 0.8524\pi$), we have $\xi_c > \xi$. In Figs. 10(d)-(f), when the perfect circulator behavior appears at $k = 0.2\pi$ ($> 0.1476\pi$) and 0.8π ($< 0.8524\pi$), we have $\xi_c < \xi$.

V. CONCLUSIONS

In summary, we have studied the nonreciprocal single-photon frequency conversion in multiple CRWs, which are coupled indirectly by optomechanical interactions with two nondegenerate mechanical modes. We have demonstrated that the frequency of a single photon can be converted nonreciprocally in two CRWs. Moreover, two different single-photon circulators are proposed in the T-shaped waveguides with two or three mechanical modes. The optomechanical systems (or

mechanical modes) offers the possibility to enable nonreciprocal frequency transduction between two CRWs with distinctively different frequencies, and they allow for dynamic control of the direction of frequency conversion by tuning the phases of external driving lasers. All the proposals can be applied to integrate devices with different frequencies and simplify the construction of hybrid quantum networks.

For simplicity, in this work we do not consider the dissipative effects of the cavities. However, in reality, all the optical or microwave cavities in the CRWs interact with the environment, resulting in the reduction of the nonreciprocal single-photon frequency converting efficiency. To lower this effect, we should enhance both the coupling strength between two nearest neighboring cavities in the CRWs and the effective optomechanical coupling strengths. The photon hopping can be enhanced by decreasing the distance between neighboring cavities, and one of the most common ways to enhance effective optomechanical coupling strengths is to increase the powers of the external driving fields. In this case, the frequencies of the mechanical modes we choose must be high enough to ensure that the rotating-wave approximation is valid in the derivations. Thus, the microwave-frequency mechanical modes coupled to superconducting quantum circuit [70] and optomechanical crystal [71] are suitable to realize our nonreciprocal single-photon frequency converters.

Acknowledgement

X.-W.X. is supported by the National Natural Science Foundation of China (NSFC) under Grant No.11604096 and the Startup Foundation for Doctors of East China Jiaotong University under Grant No. 26541059. A.-X.C. is supported by NSFC under Grant No. 11365009. Y.L. is supported by NSFC under Grant No. 11421063. Y.L. and Y.-X.L. are supported by the National Basic Research Program of China (973 Program) under Grant No. 2014CB921400. Y.-X.L. is also supported by NSFC under Grants No. 61328502 and 61025022, the Tsinghua University Initiative Scientific Research Program, and the Tsinghua National Laboratory for Information Science and Technology (TNList) Cross-Discipline Foundation.

-
- [1] M. Wallquist, K. Hammerer, P. Rabl, M. Lukin, and P. Zoller, Hybrid quantum devices and quantum engineering, *Phys. Scr.* **T137**, 014001 (2009).
 - [2] Z. L. Xiang, S. Ashhab, J. Q. You, and F. Nori, Hybrid quantum circuits: Superconducting circuits interacting with other quantum systems, *Rev. Mod. Phys.* **85**, 623 (2013).
 - [3] P. Kumar, Quantum frequency conversion, *Opt. Lett.* **15**, 1476 (1990).
 - [4] J. Huang and P. Kumar, Observation of quantum frequency conversion, *Phys. Rev. Lett.* **68**, 2153 (1992).
 - [5] M. T. Rakher, L. Ma, O. Slattery, X. Tang, and K. Srinivasan, Quantum transduction of telecommunications-band single photons from a quantum dot by frequency upconversion, *Nat. Photon.* **4**, 786 (2010).
 - [6] R. Ikuta, Y. Kusaka, T. Kitano, H. Kato, T. Yamamoto, M. Koashi, and N. Imoto, Wide-band quantum interface for visible-to-telecommunication wavelength conversion. *Nat. Commun.* **2**, 537 (2011).
 - [7] S. Zaske, A. Lenhard, C. A. Keßler, J. Kettler, C. Hepp, C. Arend, R. Albrecht, W.-M. Schulz, M. Jetter, P. Michler, and C. Becher, Visible-to-Telecom Quantum Frequency Conversion of Light from a Single Quantum Emitter, *Phys. Rev. Lett.* **109**, 147404 (2012).
 - [8] S. Ates, I. Agha, A. Gulinatti, I. Rech, M. T. Rakher, A. Badolato, and K. Srinivasan, Two-Photon Interference Using Background-Free Quantum Frequency Conversion of Sin-

- gle Photons Emitted by an InAs Quantum Dot, *Phys. Rev. Lett.* **109**, 147405 (2012).
- [9] B. Abdo, K. Sliwa, F. Schackert, N. Bergeal, M. Hatridge, L. Frunzio, A. D. Stone, and M. Devoret, Full Coherent Frequency Conversion between Two Propagating Microwave Modes, *Phys. Rev. Lett.* **110**, 173902 (2013).
- [10] H. J. McGuinness, M. G. Raymer, C. J. McKinstrie, and S. Radic, Quantum Frequency Translation of Single-Photon States in a Photonic Crystal Fiber, *Phys. Rev. Lett.* **105**, 093604 (2010).
- [11] A. G. Radnaev, Y. O. Dudin, R. Zhao, H. H. Jen, S. D. Jenkins, A. Kuzmich, and T. A. B. Kennedy, A quantum memory with telecom-wavelength conversion, *Nat. Phys.* **6**, 894 (2010).
- [12] D. Farnesi, A. Barucci, G. C. Righini, S. Berneschi, S. Soria, and G. N. Conti, Optical Frequency Conversion in Silica-Whispering-Gallery-Mode Microspherical Resonators, *Phys. Rev. Lett.* **112**, 093901 (2014).
- [13] Y. X. Liu, H. C. Sun, Z. H. Peng, A. Miranowicz, J. S. Tsai, and F. Nori, Controllable microwave three-wavemixing via a single three-level superconducting quantum circuit, *Sci. Rep.* **4**, 7289 (2014).
- [14] Y. J. Zhao, J. H. Ding, Z. H. Peng, Y. X. Liu, Realization of microwave amplification, attenuation, and frequency conversion using a single three-level superconducting quantum circuit, *Phys. Rev. A* **95**, 043806 (2017).
- [15] A. F. Kockum, V. Macrì, L. Garziano, S. Savasta, and F. Nori, Frequency conversion in ultrastrong cavity QED, *Sci. Rep.* **7**, 5313 (2017).
- [16] M. Bradford, K. C. Obi, and J. T. Shen, Efficient Single-Photon Frequency Conversion Using a Sagnac Interferometer, *Phys. Rev. Lett.* **108**, 103902 (2012).
- [17] M. Bradford and J. T. Shen, Single-photon frequency conversion by exploiting quantum interference, *Phys. Rev. A* **85**, 043814 (2012).
- [18] W. B. Yan, J. F. Huang, and H. Fan, Tunable single-photon frequency conversion in a Sagnac interferometer, *Sci. Rep.* **3**, 3555 (2013).
- [19] L. Zhou, L. P. Yang, Y. Li, and C. P. Sun, Quantum Routing of Single Photons with a Cyclic Three-Level System, *Phys. Rev. Lett.* **111**, 103604 (2013).
- [20] Z. H. Wang, L. Zhou, Y. Li, and C. P. Sun, Controllable single-photon frequency converter via a one-dimensional waveguide, *Phys. Rev. A* **89**, 053813 (2014).
- [21] T. J. Kippenberg and K. J. Vahala, Cavity Optomechanics: Back-Action at the Mesoscale, *Science* **321**, 1172 (2008).
- [22] F. Marquardt and S. M. Girvin, Optomechanics, *Physics* **2**, 40 (2009).
- [23] M. Aspelmeyer, P. Meystre, and K. Schwab, Quantum optomechanics, *Phys. Today* **65**(7), 29 (2012).
- [24] M. Aspelmeyer, T. J. Kippenberg, and F. Marquardt, Cavity Optomechanics, *Rev. Mod. Phys.* **86**, 1391 (2014).
- [25] M. Metcalfe, Applications of cavity optomechanics, *Appl. Phys. Rev.* **1**, 031105 (2014).
- [26] A. H. Safavi-Naeini and O. Painter, Proposal for an optomechanical traveling wave phonon/photon translator, *New J. Phys.* **13**, 013017 (2011).
- [27] Y. D. Wang and A. A. Clerk, Using Interference for High Fidelity Quantum State Transfer in Optomechanics, *Phys. Rev. Lett.* **108**, 153603 (2012).
- [28] L. Tian, Adiabatic State Conversion and Pulse Transmission in Optomechanical Systems, *Phys. Rev. Lett.* **108**, 153604 (2012).
- [29] J. T. Hill, A. H. Safavi-Naeini, J. Chan, and O. Painter, Coherent optical wavelength conversion via cavity optomechanics, *Nat. Commun.* **3**, 1196 (2012).
- [30] Y. Liu, M. Davanco, V. Aksyuk, and K. Srinivasan, Electromagnetically Induced Transparency and Wideband Wavelength Conversion in Silicon Nitride Microdisk Optomechanical Resonators, *Phys. Rev. Lett.* **110**, 223603 (2013).
- [31] C. Dong, V. Fiore, M. C. Kuzyk, L. Tian, and H. Wang, Optical wavelength conversion via optomechanical coupling in a silica resonator, *Ann. Phys. (Berlin)* **527**, 100 (2015).
- [32] F. Lecocq, J. B. Clark, R. W. Simmonds, J. Aumentado, and J. D. Teufel, Mechanically Mediated Microwave Frequency Conversion in the Quantum Regime, *Phys. Rev. Lett.* **116**, 043601 (2016).
- [33] J. Bochmann, A. Vainsencher, D. D. Awschalom, and A. N. Cleland, Nanomechanical coupling between microwave and optical photons, *Nature Phys.* **9**, 712 (2013);
- [34] T. Bağcı, A. Simonsen, S. Schmid, L. G. Villanueva, E. Zeuthen, J. Appel, J. M. Taylor, A. Sørensen, K. Usami, A. Schliesser, and E. S. Polzik, Optical detection of radio waves through a nanomechanical transducer, *Nature (London)* **507**, 81 (2014).
- [35] R. W. Andrews, R. W. Peterson, T. P. Purdy, K. Cicak, R. W. Simmonds, C. A. Regal, and K. W. Lehnert, Bidirectional and efficient conversion between microwave and optical light, *Nature Phys.* **10**, 321 (2014).
- [36] A. Rueda, F. Sedlmeir, M. C. Collodo, U. Vogl, B. Stiller, G. Schunk, D. V. Strekalov, C. Marquardt, J. M. Fink, O. Painter, G. Leuchs, and H. G. L. Schwefel, Efficient microwave to optical photon conversion: an electro-optical realization, *Optica* **3**, 000597 (2016).
- [37] D. Jalas, A. Petrov, M. Eich, W. Freude, S. Fan, Z. Yu, R. Baets, M. Popović, A. Melloni, J. D. Joannopoulos, M. Vanwolleghem, C. R. Doerr, and H. Renner, What is - and what is not - an optical isolator, *Nat. Photon.* **7**, 579 (2013).
- [38] J. Koch, A. A. Houck, K. L. Hur, and S. M. Girvin, Time-reversal-symmetry breaking in circuit-QED-based photon lattices, *Phys. Rev. A* **82**, 043811 (2010).
- [39] S. J. M. Habraken, K. Stannigel, M. D. Lukin, P. Zoller, and P. Rabl, Continuous mode cooling and phonon routers for phononic quantum networks, *New J. Phys.* **14**, 115004 (2012).
- [40] L. Ranzani and J. Aumentado, A geometric description of non-reciprocity in coupled two-mode systems, *New J. Phys.* **16**, 103027 (2014).
- [41] L. Ranzani and J. Aumentado, Graph-Based Analysis of Nonreciprocity in Coupled-Mode Systems, *New J. Phys.* **17**, 023024 (2015).
- [42] Y. P. Wang, W. Wang, Z. Y. Xue, W. L. Yang, Y. Hu, and Y. Wu, Realizing and characterizing chiral photon flow in a circuit quantum electrodynamics necklace, *Sci. Rep.* **5**, 8352 (2015).
- [43] K. M. Sliwa, M. Hatridge, A. Narla, S. Shankar, L. Frunzio, R. J. Schoelkopf, and M. H. Devoret, Reconfigurable Josephson Circulator/Directional Amplifier, *Phys. Rev. X* **5**, 041020 (2015).
- [44] M. Schmidt, S. Kessler, V. Peano, O. Painter, and F. Marquardt, Optomechanical creation of magnetic fields for photons on a lattice, *Optica* **2**, 635 (2015).
- [45] A. Metelmann and A. A. Clerk, Nonreciprocal Photon Transmission and Amplification via Reservoir Engineering, *Phys. Rev. X* **5**, 021025 (2015).
- [46] X. W. Xu and Y. Li, Optical nonreciprocity and optomechanical circulator in three-mode optomechanical systems, *Phys. Rev. A* **91**, 053854 (2015).
- [47] K. Fang, M. H. Matheny, X. Luan, and O. Painter, Optical transduction and routing of microwave phonons in cavity-optomechanical circuits, *Nat. Photon.* **10**, 489 (2016).
- [48] X. Xu and J. M. Taylor, Optomechanically-induced chiral trans-

- port of phonons in one dimension, arXiv:1701.02699 [quant-ph].
- [49] F. X. Sun, D. Mao, Y. T. Dai, Z. Ficek, Q. Y. He, and Q. H. Gong, Phase control of entanglement and quantum steering in a three-mode optomechanical system, arXiv:1706.04474 [quant-ph].
- [50] F. Ruesink, M.-A. Miri, A. Alù, and E. Verhagen, Nonreciprocity and magnetic-free isolation based on optomechanical interactions. *Nat. Commun.* **7**, 13662 (2016).
- [51] K. Fang, J. Luo, A. Metelmann, M. H. Matheny, F. Marquardt, A. A. Clerk, O. Painter, Generalized non-reciprocity in an optomechanical circuit via synthetic magnetism and reservoir engineering, *Nature Physics* (2017) (Published online) doi:10.1038/nphys4009.
- [52] X. W. Xu, Y. Li, A. X. Chen, and Y. X. Liu, Nonreciprocal conversion between microwave and optical photons in electro-optomechanical systems, *Phys. Rev. A* **93**, 023827 (2016).
- [53] A. Metelmann and A. A. Clerk, Non-reciprocal quantum interactions and devices via autonomous feed-forward, *Phys. Rev. A* **95**, 013837 (2017).
- [54] L. Tian and Z. Li, Nonreciprocal quantum-state conversion between microwave and optical photons, *Phys. Rev. A* **96**, 013808 (2017).
- [55] M.-A. Miri, F. Ruesink, E. Verhagen, and A. Alù, Optical Non-reciprocity Based on Optomechanical Coupling, *Phys. Rev. Applied* **7**, 064014 (2017).
- [56] N. R. Bernier, L. D. Tóth, A. Koottandavida, A. Nunnenkamp, A. K. Feofanov, T. J. Kippenberg, Nonreciprocal reconfigurable microwave optomechanical circuit, arXiv:1612.08223 [quant-ph].
- [57] G. A. Peterson, F. Lecocq, K. Cicak, R. W. Simmonds, J. Aumentado, and J. D. Teufel, Demonstration of efficient nonreciprocity in a microwave optomechanical circuit, *Phys. Rev. X* **7**, 031001 (2017).
- [58] S. Barzanjeh, M. Wulf, M. Peruzzo, M. Kalae, P. B. Dieterle, O. Painter, and J. M. Fink, Mechanical On-Chip Microwave Circulator, arXiv:1706.00376 [quant-ph].
- [59] X. W. Xu, A. X. Chen, Y. Li, and Yu-xi Liu, Single-photon nonreciprocal transport in one-dimensional coupled-resonator waveguides, *Phys. Rev. A* **95**, 063808 (2017).
- [60] S. Yang, Z. Song, and C. P. Sun, Asymmetric transmission through a flux-controlled non-Hermitian scattering center, arXiv:0912.0324 [quant-ph].
- [61] X. Q. Li, X. Z. Zhang, G. Zhang, and Z. Song, Asymmetric transmission through a flux-controlled non-Hermitian scattering center, *Phys. Rev. A* **91**, 032101 (2015).
- [62] A. Wallraff, D. I. Schuster, A. Blais, L. Frunzio, R. S. Huang, J. Majer, S. Kumar, S. M. Girvin, and R. J. Schoelkopf, Strong coupling of a single photon to a superconducting qubit using circuit quantum electrodynamics, *Nature (London)* **431**, 162 (2004).
- [63] M. J. Hartmann, F. G. S. L. Brandão, and M. B. Plenio, Strongly interacting polaritons in coupled arrays of cavities, *Nat. Phys.* **2**, 849 (2006).
- [64] M. A. Castellanos-Beltran and K. W. Lehnert, Widely tunable parametric amplifier based on a superconducting quantum interference device array resonator, *Appl. Phys. Lett.* **91**, 083509 (2007)
- [65] M. Notomi, E. Kuramochi, and T. Tanabe, Large-scale arrays of ultrahigh-Q coupled nanocavities, *Nat. Photon.* **2**, 741 (2008).
- [66] I. Wilson-Rae, N. Nooshi, W. Zwerger, and T. J. Kippenberg, Theory of Ground State Cooling of a Mechanical Oscillator Using Dynamical Backaction, *Phys. Rev. Lett.* **99**, 093901 (2007).
- [67] F. Marquardt, J. P. Chen, A. A. Clerk, and S. M. Girvin, Quantum Theory of Cavity-Assisted Sideband Cooling of Mechanical Motion, *Phys. Rev. Lett.* **99**, 093902 (2007).
- [68] Y. Li, Y. D. Wang, F. Xue, and C. Bruder, Quantum theory of transmission line resonator-assisted cooling of a micromechanical resonator, *Phys. Rev. B* **78**, 134301 (2008).
- [69] X. W. Xu, Y. X. Liu, C. P. Sun, and Y. Li, Mechanical \mathcal{PT} symmetry in coupled optomechanical systems, *Phys. Rev. A* **92**, 013852 (2015).
- [70] A. D. O'Connell, M. Hofheinz, M. Ansmann, R. C. Bialczak, M. Lenander, E. Lucero, M. Neeley, D. Sank, H. Wang, M. Weides, J. Wenner, J. M. Martinis, and A. N. Cleland, Quantum ground state and single-phonon control of a mechanical resonator, *Nature (London)* **464**, 697 (2010).
- [71] A. H. Safavi-Naeini, J. T. Hill, S. Meenehan, J. Chan, S. Gröblacher, and O. Painter, Two-Dimensional Phononic-Photonic Band Gap Optomechanical Crystal Cavity, *Phys. Rev. Lett.* **112**, 153603 (2014).